Applied Physics Express **11**, 092001 (2018)
https://doi.org/**10.7567/APEX.11.092001**

Asymmetric light reflectance by Fano resonance between Fresnel reflection and localized surface plasmons

He Wang[1], Penggang Li[1], Na Gao[1*], Kai Huang[1*], Junyong Kang[1], Li Ji[2], and Edward Yu[2]

[1]*Fujian Provincial Key Laboratory of Semiconductors and Applications, Collaborative Innovation Center for Optoelectronic Semiconductors and Efficient Devices, Department of Physics, Xiamen University, Xiamen 361005, P. R. China*
[2]*Department of Electrical and Computer Engineering, Microelectronic Research Centre, The University of Texas at Austin, Austin, TX 78758, U.S.A.*

[*]E-mail: ngao@xmu.edu.cn; k_huang@xmu.edu.cn

Received June 22, 2018; accepted July 11, 2018; published online July 30, 2018

The asymmetric light reflectance behavior arising from the Fano interference between Fresnel reflection and localized surface plasmons (LSPs) is investigated. Finite-difference time-domain (FDTD) simulation results demonstrate that, when light is incident from air, reflectance spectra show peaks at the LSP resonance wavelength regardless of the metal nanoparticle density. When light is incident from the substrate, reflectance spectra show typical Fano profiles. This phenomenon can be attributed to different reflectance phase shifts induced when light is incident from different directions. Experiments are conducted with Ag-nanoparticle-coated quartz wafers. The measured spectra are in good agreement with the simulated results. © 2018 The Japan Society of Applied Physics

In 1961, in a quantum mechanical study of the autoionizing states of atoms, Fano discovered a new type of resonance, *Fano resonance*, arising from the constructive and destructive interferences of a narrow discrete (Lorentzian) resonance with a continuum.[1)] Fano resonance, a wave interference phenomenon, is also applied to classical optics systems, such as prism-coupled micropillars[2)] and photonic crystals.[3)] In particular, over the past few years, Fano resonances have been observed in a number of plasmonic nanostructures,[4–7)] along with metamaterials, plasmonic-nanostructure constituents, including diffraction gratings,[8)] holes,[9)] and particle arrays.[10–12)]

Localized surface plasmon (LSP) resonances originate from the collective oscillation of free electrons that are confined within a metal nanoparticle (NP) when coupled with light.[13,14)] LSPs have attracted tremendous interest for a wide range of applications such as sensors,[15,16)] optical imaging,[17,18)] light-emitting diodes (LEDs),[19,20)] solar cells,[21,22)] and photodetectors.[23,24)] The particle polarizability of LSPs has a typical Lorentzian form;[25)] thus, Fano resonance may also occur when LSPs interfere with other wave states. For example, asymmetric quadrupole or octupole Fano resonances observed in a solid metallic nanosphere can be attributed to the interference between narrow and broad resonances.[26)] In particular, for most applications, the use of substrates is unavoidable. It has been revealed that the interference between the LSP resonance and the Fresnel reflection continuum results in a highly asymmetric reflectance spectrum for metallic NP arrays on dielectric substrates.[27,28)] In our previous study, we reported and analyzed an asymmetric light reflectance from metal NP arrays on dielectric surfaces.[29)] Results of the experiment and theoretical analysis demonstrated that, when light is reflected by a metal-NP-array-coated surface, the overall reflected wave can be regarded as a superposition of waves reflected by the air/dielectric interface and LSPs. When light is incident from a medium with high refractive index, the lineshape of the reflectance spectrum changes from a dip to a peak as the NP density increases. Moreover, when light is incident from a medium with low refractive index, reflectance spectra show peaks around the LSP resonance wavelength regardless of the NP density. However, in our previous study, only the reflectance behaviors at the LSP resonance wavelength are discussed and the lineshape of the reflectance spectra is not obtained theoretically.

In this study, we investigated the lineshape of the reflectance spectra of the interference between LSPs and dielectric interfaces by finite-difference time-domain (FDTD) simulations, theoretical analyses, and experiments. The FDTD simulations and theoretical analyses show that the phase shift of the reflectance wave is close to π and does not vary markedly with the wavelength when light is incident from air. Thus, the reflectance spectra show peaks around the LSP resonance wavelength regardless of the NP density, showing a typical constructive interference behavior. However, when light is incident from the substrate, the reflectance-phase shifts from 0 to $-\pi$ when the wavelength increases from 0 to λ_{LSPR} and then shifts from π to 0 when the wavelength increases from λ_{LSPR} to ∞. Thus, the interference between LSPs and interface reflection is destructive and then results in Fano lineshape reflectance spectra. On the other hand, the theoretical analyses and experiments show that the asymmetric factor q in the Fano function, which determines the lineshape of a Fano profile, increases with the NP density when the NP volume is fixed. In addition, the total amount of metal (NP volume times NP density) increases under the $q = 1$ condition when the NP volume increases.

FDTD simulations were carried out with commercial software, FDTD Solutions v8.15.736 (Lumerical Solutions). Periodic boundary conditions were considered for lateral dimensions, while for vertical dimensions, 12-layered perfectly matched layers (PMLs) were employed in order to increase the stability of the simulations. The mesh accuracy was set to 2. The incident plane wave propagated perpendicularly to the interface of two media from the z- or $-z$-direction with the same incident energy density. The polarization direction of the incident wave was set along the x-direction. The metal dielectric function of silver was obtained from the handbook of Chemistry and Physics (CRC handbook), and the refractive index of quartz was set to 1.5. A series of samples were produced to prove the simulated results experimentally. Ag NPs were fabricated on quartz wafers (0.5 mm thick). The quartz wafers were ultrasonically degreased in acetone, ethanol, and then doubly deionized water for 3 min

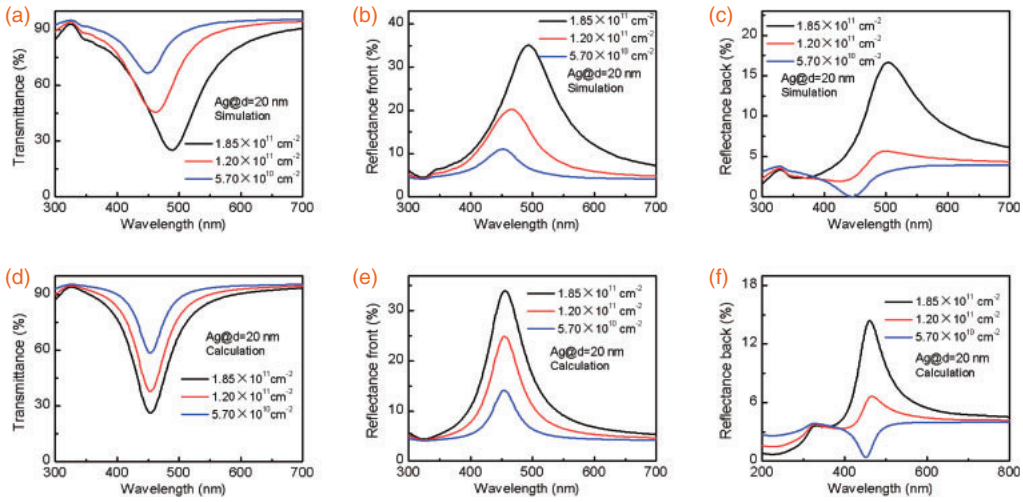

Fig. 1. (a) FDTD-simulated transmittance spectra of the hemispherical Ag NPs with different NP densities on quartz substrates. (b, c) FDTD-simulated reflectance spectra when light is normally incident from the air and substrate, respectively. (d) Calculated transmittance spectra using Eq. (1). (e) and (f) Calculated reflectance spectra when light is normally incident from the air and substrate using Eq. (1), respectively. The diameter of the Ag NPs for all simulations and calculations is 20 nm.

each. Ag films with thicknesses of approximately 2, 4, and 6 nm were sputtered by using a SCD005 sputtering system (Balzers Union, Balzers, Liechtenstein). The samples were then annealed under N_2 by rapid thermal annealing at 450 °C for 60 s to form Ag NP arrays.

Figure 1(a) shows the FDTD-simulated transmittance spectra of 20-nm-diameter Ag NP arrays with different NP densities on quartz substrates. It is clearly observed that the transmittance dips shown in all spectra correspond to the LSP resonance wavelengths. The transmittance dips redshift when the NP density increases, which can be attributed to the coupling between adjacent Ag NPs.[30–32] Figures 1(b) and 1(c) show the simulated reflectance spectra of Ag NP arrays with different NP densities on quartz substrates when light is incident from different directions. In Fig. 1(b), we show that, when light is incident from air, the reflectance spectra show peaks at the LSP resonance wavelengths, independent of the NP density. The peak intensity increases when the NP density increases. Note that, for the whole wavelength regime of all spectra, the reflectance intensities are higher than 4%, which corresponds to the reflectance intensities of quartz, showing a typical constructive interference behavior. However, when light is incident from the substrate [Fig. 1(c)], the reflectance spectra show valleys or peaks when the NP density is relatively low or high, respectively. For intermediate NP densities (around 1200 μm^{-2} in our simulations), the lineshape of the reflectance spectrum is highly asymmetric. There are one valley and one peak shown in the spectrum at wavelengths shorter and longer than the LSP resonance wavelength, respectively. Note that the valley minima and peak maxima are smaller and higher than 4%, showing asymmetric constructive and destructive interference phenomena located very close to each other, respectively. This phenomenon can be explained by the interference between the LSP resonance of metal NPs and a continuum caused by the reflection from the air/dielectric interface, which is the so-called Fano resonance.[1,27] By using a model based on modified Fresnel coefficients, the transmitted intensity T and the reflectance intensity R for a normally incident wave of unity amplitude can be written as[33,34]

$$T = \frac{4n_i n_t}{\left| n_i + n_t - i\frac{\omega}{c}\rho\alpha(\omega)_{MLWA} \right|^2},$$

$$R = |r|^2 = \left| \frac{n_i - n_t + i\frac{\omega}{c}\rho\alpha(\omega)_{MLWA}}{n_i + n_t - i\frac{\omega}{c}\rho\alpha(\omega)_{MLWA}} \right|^2, \quad (1)$$

where n_i and n_t are the refractive indices of the incidence and transmittance media, respectively, and $\rho\alpha(\omega)_{MLWA}$ defines the total optical density of the interface through the frequency-dependent polarizability with the modified long wavelength approximation, $\alpha(\omega)_{MLWA}$, of a single NP and the surface density of NPs, ρ. By assuming that the metal dielectric function is given by the CRC handbook, it can be shown that the polarizability takes an essentially Lorentzian form:[27,35]

$$\alpha(\omega)_{MLWA} = \frac{\alpha(\omega)}{1 - \frac{k^2}{4\pi r}\alpha(\omega) - i\frac{k^3}{6\pi}\alpha(\omega)}, \quad (2)$$

where

$$\alpha(\omega) = \frac{V[\varepsilon(\omega) - \varepsilon_{eff}]}{\varepsilon_{eff} + L[\varepsilon(\omega) - \varepsilon_{eff}]}.$$

Here, V is the volume of the metal NPs, $L = 0.2$ is a geometrical depolarization factor,[36,37] $\varepsilon_{eff} = n_{eff}^2 = 1.69$, and $k = (\omega/c)n_{eff}$ [modified long wavelength approximation (MLWA)]. Figures 1(d)–1(f) present the transmittance spectrum T and the reflectance spectrum R calculated from Eq. (1) when light is incident from the air and substrate. The effective refractive index surrounding the Au NPs is set to 1.3, and the geometric parameter L is set to 0.2 by fitting the corresponding LSP resonance wavelength. The calculated reflectance spectra are generally in agreement with the FDTD-simulated results. However, one may observe that the calculated LSP resonance wavelength does not redshift when the NP density increases compared with the simulated spectra. This is because the coupling effect between

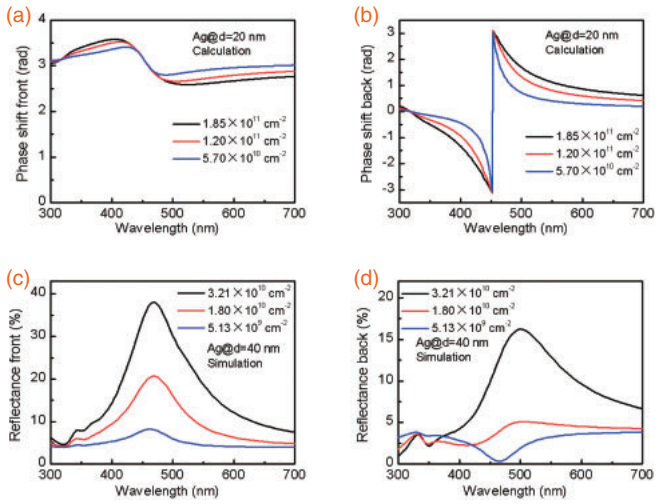

Fig. 2. (a, b) Calculated reflectance phase shift when light is incident from the air and substrate, respectively. (c, d) FDTD-simulated reflectance spectra when light is normally incident from the air and substrate, respectively. The diameter of the hemispherical Ag NPs is 40 nm.

neighboring NPs is neglected in the modified Fresnel equations.[33)]

The difference between reflectance behaviors when light is incident from different directions can be attributed to the phase shift of the reflected wave. Figures 2(a) and 2(b) present the reflection phase shift $\arg(r)$ values calculated from Eq. (1) when light is incident from the air and substrate, respectively. As shown in Fig. 2(a), when light is incident from the air, the phase shift of the reflection wave is close to π with a very small variance in wavelength. However, when light is incident from the substrate, the reflection phase shifts from 0 to $-\pi$ when the wavelength increases from 0 to λ_{LSPR} and then shifts from π to 0 when the wavelength increases from λ_{LSPR} to ∞ [Fig. 2(b)]. This can be attributed to the reflection phase of the wave reflected from the Ag NPs. From Eq. (1), we know that, at the LSP resonance wavelength, the additional term $(i\omega)/c\rho\alpha(\omega_{\mathrm{LSPR}})_{\mathrm{MLWA}}$ is a negative real number. Thus, when light is incident from the air or substrate, the interference between the wave reflected from the dielectric interface and the LSPs is constructive or destructive at the LSP resonance wavelength, respectively. Thus, when light is incident from the air, the reflectance spectra show relatively symmetric peaks regardless of the NP density. When light is incident from the substrate, the reflectance spectra show typical Fano lineshapes. In accordance with the basic Fano resonance theory,[1)] the lineshape of a Fano profile can be characterized by a Fano function,

$$I = \frac{(\varepsilon + q)^2}{\varepsilon^2 + 1}, \tag{3}$$

using the phenomenological asymmetry parameter q and the reduced energy ε defined by $2(E - E_{\mathrm{F}})/\Gamma$. E_{F} is the resonant energy and Γ is the width of the discrete state, i.e., the LSP state in our case. One can see that, when the NP density is $1.85 \times 10^{11}\,\mathrm{cm}^{-2}$, q is relatively large, when the NP density is $5.70 \times 10^{10}\,\mathrm{cm}^{-2}$, q is relatively small, and when the NP density is close to $1.20 \times 10^{11}\,\mathrm{cm}^{-2}$, q is close to 1.

Equations (1) and (3) show that q is primarily related to the term $i\omega\rho\alpha(\omega)_{\mathrm{MLWA}}/c$. In Eq. (2), both the total amount of metal, ρV (in unit of thickness), and the volume of individual metal NPs, V, will affect the q of the reflectance spectra when light is incident from the substrate. Figures 2(c) and 2(d) show the simulated and calculated reflectance spectra for the Ag NPs of 40 nm diameter when light is incident from the air and substrate, respectively. It is clearly observed that q is close to 1 when the NP density is close to $1.80 \times 10^{10}\,\mathrm{cm}^{-2}$. Thus, we consider that the $q = 1$ condition occurs when $\rho V =$ 2.4 and 3.0 nm for Ag NPs with diameters of 20 and 40 nm, respectively. From Eq. (2), we determine that, when the NP volume increases, the imaginary part in the denominator increases. Thus, the modulus of a decreases and a larger ρV is needed for the $q = 1$ condition.

These results have been verified experimentally via measurements of transmittance and reflectance for samples with Ag NP arrays with different sizes and densities on quartz substrates. Figures 3(a)–3(c) show typical SEM images of the Ag NP arrays formed by annealing from Ag films with thicknesses of 2, 4, and 6 nm (denoted as samples A, B, and C), respectively. The average diameters of Ag NPs are 24, 32, and 80 nm, and the NP densities are 1.07×10^{11}, 4.58×10^{10}, and $7.5 \times 10^{9}\,\mathrm{cm}^{-2}$ for samples A, B, and C,

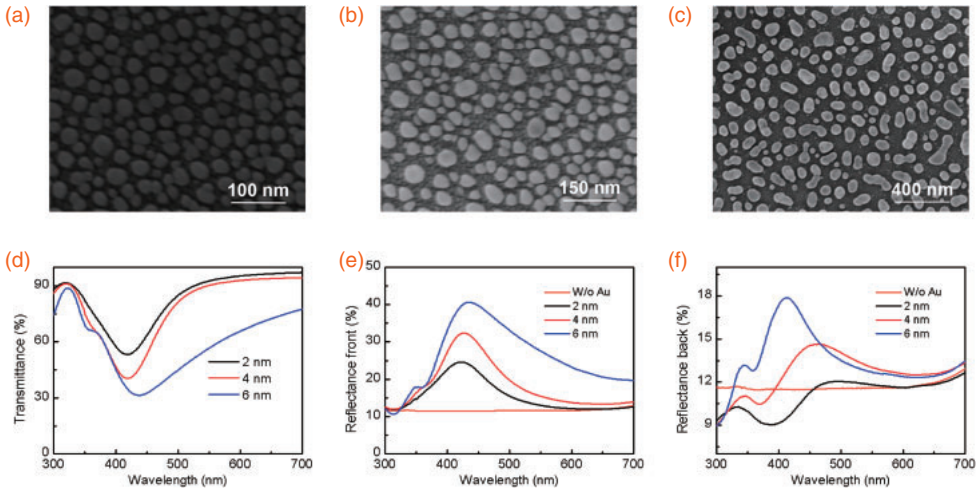

Fig. 3. (a)–(c) SEM images of the Ag NPs annealed from the Ag films with thicknesses of 2, 4, and 6 nm, respectively. (d)–(f) Measured transmittance spectra and reflectance spectra when light is incident from the air and substrates, respectively.

respectively. Figure 3(d) shows the transmittance spectra of these samples, with transmittance dip redshifts when the Ag film thickness increases. The LSP resonance wavelength redshift is primarily due to the increase in NP size rather than the decrease in separation distance between the NPs. Figure 3(e) shows the reflectance spectra of samples A–C when light is incident from the air. As predicted theoretically, the reflectance peaks at the LSP resonance wavelengths are observed in all spectra regardless of the film thickness before annealing and the whole spectra are above the reflectance spectrum of the quartz wafer without Ag NP arrays. When light is incident from the quartz substrate, the reflectance spectrum of sample A shows a dip at approximately 387 nm. The reflectance spectrum of sample B shows one dip at approximately 369 nm and one peak at approximately 464 nm. The dip and peak intensities are lower and higher than the reflectance intensity of the quartz wafer without Ag NP arrays, respectively. However, for sample C, there are two peaks at approximately 414 and 345 nm shown in the reflectance spectrum. Since the reflectance intensity between these two peaks is higher than that of the quartz wafer without Ag NP arrays, the reflectance peak at the shorter wavelength may be attributed to the quadrupole mode generated in relatively larger metal NPs. In general, these behaviors are in good agreement with the theoretical prediction shown above. From the reflectance spectra of samples A–C, q can be calculated as 0.45, 1.8, and 2.5, respectively. Thus, one can see that the $q = 1$ condition should occur for the Ag film thickness of ~3 nm before annealing, which is in good agreement with that in the simulated results.

In conclusion, we investigated lineshapes of reflectance spectra using the interference between LSPs and dielectric interfaces. FDTD simulations and theoretical analyses show that the phase shift of the reflectance wave is close to π and does not vary markedly in wavelength when light is incident from air. Thus, reflectance spectra show peaks around the LSP resonance wavelength regardless of the NP density, showing a typical constructive interference behavior. However, when light is incident from the substrate, the reflection phase shifts from 0 to $-\pi$ when the wavelength increases from 0 to λ_{LSPR} and then shifts from π to 0 when the wavelength increases from λ_{LSPR} to ∞. Thus, the interference between LSPs and interface reflection is destructive and then results in Fano lineshape reflectance spectra. FDTD simulations and theoretical analyses also suggest that the $q = 1$ condition occurs when $\rho V = 2.4$ and 3.0 nm for Ag NPs with diameters of 20 and 40 nm, respectively. A series of samples are produced to prove the simulated results experimentally. Ag NP arrays are formed by annealing Ag films with different thicknesses. Experimental results show that when the Ag film thicknesses before annealing are approximately 2, 4, and 6 nm, the reflectance spectrum when light is incident from the substrate shows a dip, an asymmetric Fano lineshape, and a peak, respectively. The $q = 1$ condition should occur for the Ag film thickness of ~3 nm before annealing. All experimental results are in good agreement with the theoretical predictions.

Acknowledgments This work was supported by the National Key Research and Development Program (2016YFB0400903), the National Natural Science Foundation of China (U1405253 and 61604124), and the fundamental research funds for the central universities (20720160018 and 20720170098).

1) U. Fano, Phys. Rev. **124**, 1866 (1961).
2) H. T. Lee and A. W. Poon, Opt. Lett. **29**, 5 (2004).
3) M. V. Rybin, A. B. Khanikaev, M. Inoue, K. B. Samusev, M. J. Steel, G. Yushin, and M. F. Limonov, Phys. Rev. Lett. **103**, 023901 (2009).
4) B. Luk'yanchuk, N. I. Zheludev, S. A. Maier, N. J. Halas, P. Nordlander, H. Giessen, and C. T. Chong, Nat. Mater. **9**, 707 (2010).
5) F. Hao, Y. Sonnefraud, P. Van Dorpe, S. A. Maier, N. J. Halas, and P. Nordlander, Nano Lett. **8**, 3983 (2008).
6) N. Verellen, Y. Sonnefraud, H. Sobhani, F. Hao, V. V. Moshchalkov, P. Van Dorpe, P. Nordlander, and S. A. Maier, Nano Lett. **9**, 1663 (2009).
7) G. Bachelier, I. Russier-Antoine, E. Benichou, C. Jonin, N. Del Fatti, F. Vallee, and P. F. Brevet, Phys. Rev. Lett. **101**, 197401 (2008).
8) A. E. Miroshnichenko, S. Flach, and Y. S. Kivshar, Rev. Mod. Phys. **82**, 2257 (2010).
9) C. Genet, M. P. van Exter, and J. P. Woerdman, Opt. Commun. **225**, 331 (2003).
10) Y. Ekinci, A. Christ, M. Agio, O. J. F. Martin, H. H. Solak, and J. F. Loffler, Opt. Express **16**, 13287 (2008).
11) L. Bossard-Giannesini, H. Cruguel, E. Lacaze, and O. Pluchery, Appl. Phys. Lett. **109**, 111901 (2016).
12) R. Nicolas, G. Leveque, J. Marae-Djouda, G. Montay, Y. Madi, J. Plain, Z. Herro, M. Kazan, P. M. Adam, and T. Maurer, Sci. Rep. **5**, 14419 (2015).
13) E. Hutter and J. H. Fendler, Adv. Mater. **16**, 1685 (2004).
14) S. Underwood and P. Mulvaney, Langmuir **10**, 3427 (1994).
15) Y. H. Fu, J. B. Zhang, Y. F. Yu, and B. Luk'yanchuk, ACS Nano **6**, 5130 (2012).
16) N. Liu, T. Weiss, M. Mesch, L. Langguth, U. Eigenthaler, M. Hirscher, C. Sonnichsen, and H. Giessen, Nano Lett. **10**, 1103 (2010).
17) L. Zhou, Q. Gan, F. J. Bartoli, and V. Dierolf, Opt. Express **17**, 20301 (2009).
18) K. Tsuboi, S. Fukuba, R. Naraoka, K. Fujita, and K. Kajikawa, Appl. Opt. **46**, 4486 (2007).
19) K. Huang, N. Gao, C. Wang, X. Chen, J. Li, S. Li, X. Yang, and J. Kang, Sci. Rep. **4**, 4380 (2014).
20) C.-H. Lu, S.-E. Wu, Y.-L. Lai, Y.-L. Li, and C.-P. Liu, J. Alloys Compd. **585**, 460 (2014).
21) J. Qi, X. Dang, P. T. Hammond, and A. M. Belcher, ACS Nano **5**, 7108 (2011).
22) X. Dang, J. Qi, M. T. Klug, P.-Y. Chen, D. S. Yun, N. X. Fang, P. T. Hammond, and A. M. Belcher, Nano Lett. **13**, 637 (2013).
23) M. Hashemi, M. Hosseini Farzad, N. A. Mortensen, and S. Xiao, Plasmonics **8**, 1059 (2013).
24) R. Jia, G. Lin, D. Zhao, Q. Zhang, X. Lin, N. Gao, and D. Liu, Appl. Surf. Sci. **332**, 340 (2015).
25) S. A. Maier, *Plasmonics: Fundamentals and Applications* (Springer, New York, 2007) p. 68.
26) M. I. Tribelsky and B. S. Luk'yanchuk, Phys. Rev. Lett. **97**, 263902 (2006).
27) M. Svedendahl and M. Kall, ACS Nano **6**, 7533 (2012).
28) M. Svedendahl, R. Verre, and M. Käll, Light: Sci. Appl. **3**, e220 (2014).
29) K. Huang, W. Pan, J. F. Zhu, J. C. Li, N. Gao, C. Liu, L. Ji, E. T. Yu, and J. Y. Kang, Sci. Rep. **5**, 18331 (2015).
30) B. M. Reinhard, M. Siu, H. Agarwal, A. P. Alivisatos, and J. Liphardt, Nano Lett. **5**, 2246 (2005).
31) Y. Lu, G. L. Liu, and L. P. Lee, Nano Lett. **5**, 5 (2005).
32) F. J. García de Abajo, J. Phys. Chem. C **112**, 17983 (2008).
33) R. Lazzari and I. Simonsen, Thin Solid Films **419**, 124 (2002).
34) D. Bedeaux and J. Vlieger, *Optical Properties of Surfaces* (Imperial College Press, London, 2002) p. 45.
35) I. Zorić, M. Zäch, B. Kasemo, and C. Langhammer, ACS Nano **5**, 2535 (2011).
36) A. Mendoza-Galván, K. Järrendahl, A. Dmitriev, T. Pakizeh, M. Käll, and H. Arwin, Opt. Express **19**, 12093 (2011).
37) C. F. Bohren and D. R. Huffman, *Absorption and Scattering of Light by Small Particles* (Wiley, New York, 1983) p. 141.